Publisher
Maharshi Charaka Ayurveda
www.maharshicharaka.in

Journal of Ayurveda and Integrated Medical Sciences

2025 Volume 10 Number 10 October

E-ISSN:2456-3110

Research Article

Alzheimer's Disease

Network Pharmacology and AI-Based Analysis of Dioscorea bulbifera Linn. in Scopolamine-Induced Memory Impairment in OVX Rats: Insights into Estrogen-Linked Alzheimer's Disease

Chowdhury MR[1], Tiwari A[2], Dubey GP[3], Vijaykumar SD[4*]

DOI:10.21760/jaims.10.10.3

[1] Mayank Roy Chowdhury, Department of Biotechnology, National Institute of Technology, Tadepalligudem, Andhra Pradesh, India.
[2] Anamika Tiwari, Department of Kriya Sharir, Institute of Medical Sciences, Banaras Hindu University, Varanasi, Uttar Pradesh, India.
[3] Govind Prasad Dubey, Department of Kriya Sharir, Institute of Medical Sciences, Banaras Hindu University, Varanasi, Uttar Pradesh, India.
[4*] Sudarshana Deepa Vijaykumar, Department of Biotechnology, National Institute of Technology, Tadepalligudem, Andhra Pradesh, India.

Alzheimer's disease (AD) is one of the leading causes of dementia characterized by cognitive decline. Women are more likely to develop (AD) than men, possibly because estrogen levels drop after menopause. This study aimed to elucidate the effect of Dioscorea bulbifera (DB) extract on scopolamine-induced memory impairment in rats and to decipher the molecular mechanism of its phytoconstituents using an integrated network pharmacology and artificial intelligence-based approach. Memory function was evaluated using the Elevated Plus Maze (EPM) and Morris Water Maze (MWM) tests. Scopolamine administration significantly increased transfer latencies in the EPM and escape latencies in the MWM compared to the control group. However, co-administration of DB extract with scopolamine reversed these effects, showing decreased transfer latencies and escape latencies, indicating improved memory. Furthermore, the DB extract restored the time spent searching the target quadrant in the MWM probe trial session, which was impaired by scopolamine. Acetylcholine (Ach) and serum estradiol levels were quantified with enzyme-linked immunosorbent assay (ELISA) on Ovx rats induced with scopolamine to have memory deficits. With predicted DB targets and a collection of AD-related genes, 132 putative targets, 68 direct regulatory targets, and 25 potential regulatory targets of DB were identified for the treatment of AD. Pathway-enrichment analysis for the potential regulatory targets indicated that neurotransmitter clearance in the synaptic cleft was pivotal in the treatment of AD with DB, molecular docking verified interactions between the core targets (ESR1, APP, GSK3β, BACE1, AChE, and MAOB) and the active ingredients.

Keywords: Alzheimer's disease, Dioscorea bulbifera, network pharmacology, molecular docking, ELISA, Hematoxylin and eosin (H&E) staining

Corresponding Author

Sudarshana Deepa Vijaykumar, Department of Biotechnology, , National Institute of Technology, Tadepalligudem, Andhra Pradesh, India.
Email:
sudarshanadeepa@nitandhra.ac.in

How to Cite this Article

Chowdhury MR, Tiwari A, Dubey GP, Vijaykumar SD, Network Pharmacology and AI-Based Analysis of Dioscorea bulbifera Linn. in Scopolamine-Induced Memory Impairment in OVX Rats: Insights into Estrogen-Linked Alzheimer's Disease. J Ayu Int Med Sci. 2025;10(10):13-34.
Available From
https://jaims.in/jaims/article/view/4323/

To Browse

Manuscript Received	Review Round 1	Review Round 2	Review Round 3	Accepted
2025-08-04	2025-08-23	2025-09-04	2025-09-13	2025-09-24

Conflict of Interest	Funding	Ethical Approval	Plagiarism X-checker	Note
None	Nil	Yes	11.25	

© 2025 by Chowdhury MR, Tiwari A, Dubey GP, Vijaykumar SD and Published by Maharshi Charaka Ayurveda Organization. This is an Open Access article licensed under a Creative Commons Attribution 4.0 International License https://creativecommons.org/licenses/by/4.0/ unported [CC BY 4.0].

Introduction

The advancements in medical science have contributed to a significant increase in the elderly population, which has led to a parallel rise in age-related neurodegenerative disorders, including dementia. Among these disorders, Alzheimer's disease (AD) stands out as the most prevalent form of dementia (Defina et al., 2013). AD is characterized by progressive cognitive decline, impacting memory, thinking, and behavior, and is associated with the presence of abnormal protein aggregates in the brain, such as amyloid-beta (Aβ) plaques and neurofibrillary tangles (NFTs) comprising hyperphosphorylated tau protein. The pathogenesis and progression of AD are influenced by several key signaling proteins. Among them, cyclin-dependent kinase-5 (CDK5), glycogen synthase kinase-3 (GSK3), and Fyn kinase play pivotal roles (Crews and Masliah, 2010). These proteins contribute to the neurodegenerative process, exacerbating the development of AD's characteristic symptoms and the degeneration of brain cells.

Alzheimer's disease (AD) is not only correlated with age but also exhibits a gender-related susceptibility, with females being at a higher risk of developing AD compared to males. This discrepancy is thought to be associated with the loss of estrogenic protection against mitochondrial toxicity induced by amyloid-β in older females. In contrast, men may be more prone to experiencing mild cognitive impairment (MCI) (Hebert et al., 2001; Musicco, 2009; Lloret and Vi, 2010; Zhu, Montagne, and Zhao, 2021).The role of estrogen in neuroprotection is carried out through several mechanisms, including its promotion of growth and development of cholinergic neurons, elevation of cholinergic activity, antioxidant properties, and its influence on the alternative metabolism of amyloid. After menopause, there is a shift in the relative concentrations of different types of estrogen, moving away from the stronger estrogen, 17-estradiol, which predominates in pre-menopausal women, and towards the weaker estrogen, estrone. Some data suggest that estrone may have more detrimental effects on cognition than 17-estradiol (Cholerton et al., 2002; Andrew and Tierney, 2018). Despite severity of Alzheimer's disease (AD), effective therapeutic interventions capable of halting disease progression or reversing its damage remain elusive.

The current treatment options consist of four FDA-approved drugs, namely Donepezil, Rivastigmine, Galantamine, and Memantine, which primarily target the cholinergic system and N-methyl-d-aspartate (NMDA) receptors. However, these medications can only provide temporary relief from symptoms rather than effectively slowing down or halting the progression of the disease (Defina et al., 2013; Knopman et al., 2021).

Dioscorea bulbifera has a long history of use in Chinese and Indian traditional medicine to address various ailments, including cancer and HIV. This plant is known for its wide range of therapeutic properties, such as analgesic, anti-inflammatory, antioxidant, diuretic, gastroprotective, antibacterial, antifungal, and hypothyroidism-fighting effects, as well as its ability to promote wound healing (Ghosh et al., 2013; Chaniad et al., 2020). The medicative significance of *Dioscorea bulbifera* is attributed to its rich phytochemical constituents, which include macromolecules, sugars, proteins, amino acids, and starch as reserve food. However, it is the presence of secondary metabolites, such as glycosides, alkaloids, tannic acids, phenolics, flavonoids, terpenoids, glucosides, steroids, and phytates/ phytic acid, that imparts its therapeutic value (Malode et al., 2015; Adeosun et al., 2016). Notably, *Dioscorea Bulbifera Linn's* flavonoid-rich fraction (FRF) has shown potent free radical scavenging properties, making it a strong antioxidant (Jayachandran, Vasanthi, and Rajamanickam, 2010).

The therapeutic benefits of *Dioscorea Bulbifera* tubers in addressing memory deficiencies in mice can be attributed to multiple mechanisms, with their notable antioxidant effects playing a crucial role. Furthermore, the plant's neuropharmacological properties present a promising avenue for potential drug discovery targeting Alzheimer's disease (Bisht Neha et al., 2013; Patel and Galani, 2017).

The previous study conducted by (Sadhu, Upadhyay, and Agrawal 2014) involved a comparison between placebo and donepezil administration with a polyherbal formulation containing extracts of *B. monnieri* (whole plant), *H. rhamnoides* (leaves and fruits), and *D. Bulbifera* (bulbils) over a period of 12 months. The results showed significant improvements in cognition and reductions in inflammation and oxidative stress in patients with senile dementia of Alzheimer's type (SDAT).

Furthermore, the study suggested that the polyherbal formulation, when combined with metformin, could be a promising therapeutic option for individuals with Type 2 Diabetes Mellitus (T2DM)-related cognitive deficits. The group receiving the polyherbal formulation demonstrated considerable enhancements in neuropsychological measures, including learning and memory skills (Dubey et al., 2015). Additionally, a study conducted by (Upadhyay et al. 2018) reaffirmed the neuroprotective effects of the formulation using scopolamine-induced memory-impaired rat models. The study revealed that the formulation could effectively reverse the memory deficit. While the exact basis for its activity was not yet fully understood, the study highlighted the importance of the molecule Diosgenin in the formulation's effects.

Diosgenin, a steroidal sapogenin, has shown great promise as a therapeutic agent for a wide range of disorders, including cancer, hypercholesterolemia, inflammation, and various infections. Its importance extends to serving as a key starting material for the synthesis of numerous steroidal drugs in the pharmaceutical industry. The therapeutic mechanisms of diosgenin are supported by its mediation of various signaling pathways (Jesus et al., 2016; Cai et al., 2020). However, it is worth noting that in rat uterotrophic assays conducted on immature rats, diosgenin does not act as an estrogen agonist, as evidenced by a study conducted through experimental validation (Ristic, Živanovic, and Šošic, 2014).

Dioscorea bulbifera contains multitude of compounds that target multiple proteins, rendering reductionist methods inadequate in fully explaining its mechanism of action. To address this complexity, the network pharmacological approach emerges as valuable tool. By employing network pharmacology, active compounds in *Dioscorea bulbifera* can be identified, and potential targets against them can be defined. Additionally, this approach allows for the prediction of molecular mechanisms based on Gene Ontology (GO) and Pathway enrichment analysis (Chandran et al., 2020; Noor et al., 2022). In a particular study, an integrative network pharmacology model was developed to investigate *Dioscorea bulbifera* molecular mechanism of action in treating Alzheimer's disease (AD). This approach helped anticipate potential targets and regulatory pathways influenced by the active components of *Dioscorea bulbifera*.

The results of this study suggest that *Dioscorea bulbifera* exerts a neuroprotective impact in the treatment of AD by modulating specific signaling pathways. The molecular basis of this action was further validated *in vivo*, providing supportive evidence for its therapeutic effects.

Materials and Methods

Screening the active components of DB

For screening bioactive compounds in *Dioscorea bulbifera* (DB), we compiled a compound library from literature reports, Traditional Chinese Medicine Integrated Database (TCMID; www.megabionet.org /tcmid/) (Huang et al., 2018), and Traditional Chinese Medicine Systems Pharmacology Database and Analysis Platform (TCMSP; http:// lsp.nwu.edu.cn/tcmsp.php) (Ru et al., 2014). Additionally, for the ADME studies, we employed SwissADME (http://www.swissadme.ch/index.php) (Daina, A., Michielin, O., & Zoete, V., 2017) and Molsoft software (https://molsoft.com/mprop/). To ensure uniqueness, duplicate compounds were removed.

The screening process considered Absorption, Distribution, Metabolism, and Excretion (ADME) characteristics, including oral bioavailability (OB), drug-likeness (DL), and Blood-Brain Barrier permeability (BBBp). OB reflects the percentage of orally administered drugs that enter the systemic circulation, while DL measures structural similarity to known compounds in the Drug Bank database. Both OB and DL are vital parameters for drug discovery. BBBp evaluates the ability of compounds to cross the Blood-Brain Barrier, essential for treating Alzheimer's disease. Compounds with BBBp below -0.3 do not penetrate the BBB, those between -0.3 and 0.3 have moderate penetration, and those above 0.3 exhibit strong penetration.

Active compounds were identified using thresholds of OB ≥ 30%, DL ≥ 0.18, and BBBp ≥ -0.3. Lipinski's Rule of 5 was applied for compounds with missing data, where molecular weight (MWT) greater than 500, computed Log P (CLogP) greater than five (or MlogP > 4.15), more than five H-bond donors, or ten H-bond acceptors may indicate poor absorption or penetration (Lipinski et al., 2001). Neuroprotective compounds affecting the central nervous system were also considered active, regardless of meeting the above criteria.

Target Prediction and disease association mining

The prediction of target proteins was accomplished using two distinct tools: the 'SwissTargetPrediction' tool (http://www.swisstargetprediction.ch/?) (Daina, Michielin, and Zoete, 2019) & 'BindingDB' database (https://www.bindingdb.org/bind/index.jsp) (Liu et al., 2007). These tools utilize artificial intelligence-based machine learning algorithms to predict target-protein interactions based on bioactive structures in (.sdf) files. The algorithms analyze patterns and features in the structures, allowing efficient and accurate predictions of potential target-protein associations. Targets with high prediction scores between 0.9 to 1 (BindingDB) and the top fifteen compounds (Swisstargetprediction) were carefully selected for further analysis while removing duplicates. To maintain a polypharmacological model for drug discovery, targets interacting with two or more bioactive compounds were prioritized, resulting in 132 putative targets. These targets were then subjected to the 'DisGeNET' server (https://www.disgenet.org/) for disease association mining, utilizing the Gene Disease Association (GDA) score to rank the degree of target-disease association (Pi et al., 2020).

Protein-Protein interaction mapping

To explore protein-protein interactions comprehensively, we employed a robust computational approach in our study. Leveraging the STRING v11.5 database (https://string-db.org/) (Szklarczyk et al., 2021), which integrates diverse data sources, including experimental evidence and computational predictions, we identified first-degree interactors of the target protein. To construct the Protein-Protein interaction (PPi) map, we focused on high-confidence interactions (score >= 0.7) and removed duplicate edges to ensure data accuracy.

The MCL (Markov Cluster) algorithm efficiently organized proteins into modules based on connectivity patterns, unveiling functional associations within the PPi map. For further analysis, we imported the PPi map into Cytoscape, where we employed the degree centrality metric to identify essential nodes (proteins) based on their direct interactions. This approach allowed us to gain valuable insights into the functional and regulatory aspects of the target protein and its associated interactors.

Network construction and analysis

Utilizing the data representing bioactive-target interactions (Table S2) and target-disease associations (Table S3), two bipartite networks were constructed using Cytoscape v3.7.1 (Shannon et al., 2003). The first bipartite network visualized the relationships between bioactive compounds and their corresponding target proteins, revealing valuable insights into target modulation and the impact of specific compounds on biological functions. The second bipartite network focused on predicting potential targets and their associations with cognitive disorders. Both constructed networks underwent topological analysis using the degree centrality parameter within Cytoscape's 'Network Analyzer' tool (https://cytoscape.org/). This approach facilitated the identification of highly influential targets and essential compounds, offering valuable information about their potential roles in the context of cognitive disorders.

Identification of Potential Regulatory Targets (PRTs) for AD Treatment

The targets associated with AD, neurodegeneration, and cognitive disorders were defined as direct regulatory targets (DRTs) (Table S3). Gene subset data from the top 50 highly modulated targets (targets with the highest number of interactions with the bioactive compounds in DB), targets with the strongest gene-disease association (GDA) score from the 'DisGeNET' server output, and top PPi node degree at 0.7 confidence were combined.

Through the intersection of these three subsets, genes considered to be crucial for the neuroprotective molecular action of DB were identified and defined as potential regulatory targets (PRTs) for AD treatment. A Venn diagram facilitated the identification of this gene subset. The PRTs were subsequently subjected to Gene Ontology and Pathway enrichment analysis to gain deeper insights into their functional significance.

Gene Ontology and Pathway enrichment analysis

The genes identified as PRTs were annotated using GO enrichment analysis with FunRich 3.1.3, a powerful tool that leverages AI and machine learning algorithms to elucidate gene activities based on biological processes, cellular components, and molecular functions (Fonseka et al., 2021).

Through AI-driven data analysis, FunRich provides a comprehensive understanding of the functional implications of the PRTs in the context of AD. Furthermore, a pathway enrichment analysis was conducted using FunRich 3.1.3, which harnesses advanced ML techniques to gain deeper insights into the signaling pathways influenced by the PRTs. The integration of AI-driven pathway enrichment analysis facilitated the identification of key biological pathways crucial for DB's therapeutic effects on AD. To validate the predicted mechanisms, in vivo testing was carried out, confirming the significant role of the PRTs and their enriched pathways in the management of AD.

Molecular Docking

The top PRTs were selected, and compounds potentially regulating these targets were reviewed. Protein crystal structures with bound inhibitors were retrieved from the Protein Data Bank (PDB). Protein preparation in Maestro (version 13.3.121) involved filling missing side chains, optimizing H-bond assignments, and performing minimization using the OPLS 2005 (Optimized Potential for Liquid Simulation) force field. Ligands were obtained from PubChem (https://pubchem.ncbi.nlm.nih.gov/) (Kim et al., 2021) using the given PubChem IDs. LigPrep was utilized to import and prepare the ligands with the same force field at pH 7.0 ± 0.4, considering possible tautomer for each ligand. Maestro allowed the utilization of grid information from already bound ligands in complexes. For unavailable complexes, grid information from the prepared protein was employed alongside prepared ligands in the Glide module. Protein-ligand docking utilized a more precise approach called extra precision in Glide. The compounds served as ligands, and the proteins corresponding to the PRTs acted as receptors for molecular docking. The results were analyzed and interpreted using Pymol software (https://pymol.org/2/).

Experimental Validation

Experimental Animals

The animal experimentation was conducted on healthy female Wistar albino rats (N=36; 10–11-week-old; 170-250 gm) obtained from the central animal house at the Institute of Medical Sciences, Banaras Hindu University, Varanasi, Uttar Pradesh, India. The study received prior approval from the institutional animal ethical committee.

The rats were housed in cages containing sterile paddy husk as bedding in controlled animal house environment with regulated temperature of (22±3 ℃) and humidity of (55± ℃). They were maintained under 12-hour light/dark cycle and provided ad libitum access to food and water. Before the experiments commenced, 7-day acclimatization period was allowed for the animals to adapt to the laboratory conditions. The experiments were conducted between 9.30 am to 5.00 pm. Each animal was used only in one experiment, and double distilled water was used for all procedures.

Drugs and reagents for animal experimentation

Dried tubers of *Dioscorea bulbifera Linn*. were collected from Gola Dinanath Market in Varanasi. Prof. N.K Dubey from Banaras Hindu University authenticated the plant (voucher specimen: Varahikand, *Dioscorea bulbifera Linn*.2018/1). Tubers were air-dried, pulverized into powder, and extracted in a soxhlet apparatus using a hydro-alcoholic solvent. The concentrated extract was stored at 4 °C. All chemical reagents and solvents were of analytical grade from Techno. Cam India. Ketamine and xylazine were used for anesthesia. Scopolamine hydrobromide induced memory impairment. Hydro-alcoholic *Dioscorea bulbifera* (Tubers) extract was used for treatment. Estradiol served as the standard drug (positive control), and its levels were analyzed using an ELISA kit (Novous biological, CATA. No. KB1794).

Ovx Surgery

Initiating the experimental procedure, a surgical ovariectomy was performed under anesthesia induced by ketamine and xylazine. The successful induction of anesthesia was confirmed by a reduced respiratory rate and lack of response to gentle pinching of the footpad. Following a previously established method (Li et al., 2014), the ovaries were meticulously removed through an abdominal incision, ensuring the induction of the desired hormonal changes required for the experimental study. Subsequently, the animals were closely monitored for a smooth post-operative recovery.

Animal grouping and drug administration

The rats were then given 84 days to develop menopausal-like conditions. After this period, the animals were randomly assigned into six groups (n=6 each) as detailed in **Table 1**.

All animals were subjected to exteroceptive behavioral memory tests using the elevated plus maze and Morris water maze. Serum 17 beta-estradiol (E2) levels and fasting plasma insulin levels were measured on days 0, 7, 14, and 28 of the treatment. Additionally, estrogen receptor-alpha (ER-α) protein expression in the uterus was evaluated. At the end of the experiment, the rats were euthanized with an overdose of chloroform. Their brains were isolated to measure acetylcholinesterase enzyme activity levels in the frontal cortex and hippocampus.

Table 1: Experimental Study Design

Groups	Animals (n=6)	Treatment	Representation
Group 1	Ovx Control	OVX + Received normal food and water	Postmenopausal
Group 2	Negative Control	OVX + Scopolamine (2 mg/kgbw/day; IP)	Late menopause
Group 3	Positive Control	OVX + Scopolamine + Donepezil (3 mg mg/kgbw/day) + Estradiol valerate (20 µg/kgbw/day IP)	Standard drug treatment
Group 4	DB 200	OVX + Scopolamine + DBME (200mg/kgbw/day)	Low Dose DB treatment
Group 5	DB 400	OVX + Scopolamine + DBME (400mg/kgbw/day)	Medium Dose DB treatment
Group 6	DB 800	OVX + Scopolamine + DBME (800mg/kgbw/day)	High Dose DB treatment

Optimum drug dose determination

Following a comprehensive toxicity study, we meticulously determined an appropriate dose for the oral administration of *Dioscorea bulbifera* tubers extract over a three-month period. Through rigorous analysis, we observed remarkable reductions in lipofuscin content, encompassing various metals and sugars such as aluminum, mercury, copper, iron, and zinc, in a dose-dependent manner. Additionally, the acetylcholine concentration exhibited a noteworthy enhancement with increasing doses. Based on these compelling findings, we concluded fixation of dose, ensuring an optimal balance between efficacy and safety of test substance.

Elevated plus maze test

The elevated plus-maze, an experimental method to study behavioral patterns (such as sensitivity to external stimuli, exploration, anxiety, learning, and memory) in laboratory animals, was conducted following a previously reported study (Komada, Takao, and Miyakawa, 2008).

The maze consisted of four arms (two open and two closed) measuring 49 cm × 10 cm, elevated 50 cm above the ground. On the 28th day, 60 minutes after treatment, each rat was placed at the end of an open arm, and the time to enter one of the closed arms was recorded as the transfer latency, representing learning and acquisition. If the rat did not enter any closed arm within 180 seconds, it was gently guided into one of the closed arms, and the transfer latency was recorded as 180 seconds. On the subsequent day (the 29th day), i.e., 24 hours later, the transfer latency was recorded again as a parameter for memory retention. Between each session, the maze was carefully cleaned with 30% ethanol to remove any potential olfactory cues, ensuring consistent and unbiased testing conditions.

Morris water maze test

The Morris water maze tested learning and spatial memory in experimental animals without motivational stimuli. The circular pool (55 cm height, 100 cm diameter) contained opaque water (22 ± 2 °C, 30 cm height) divided into four quadrants with visual cues. A fixed platform (29 cm × 6 cm) remained in one quadrant throughout the experiment. Over four days, each animal had four learning trials of 90 seconds with a 30-second intertrial interval. On day 29 (probe trial), memory retention was assessed by removing the platform, and the time spent in the target quadrant was recorded (Komada, Takao, and Miyakawa, 2008). Conducted by the Department of Pharmacology, IMS, B.H.U, Varanasi.

Biochemical estimation

Initially, 1 ml of blood was withdrawn from the orbital region of all groups during the light phase. The blood samples were then equally divided into two parts: one collected in ethylenediamin-etetraacetic acid (EDTA)-coated tubes, and the other in plain tubes. The samples in EDTA-coated tubes were centrifuged at 2000 rpm for 20 minutes at 4 °C to separate the plasma. The isolated plasma was subsequently collected, dispensed into 1.5 ml Eppendorf tubes, and stored at –80 °C until analysis. For serum preparation, the blood samples in plain tubes were allowed to clot for 2 hours before being centrifuged at 4000 rpm for 15 minutes. Levels of estradiol (E2) and insulin were quantified using enzyme-linked immunosorbent assay (ELISA) kits, following the manufacturer's instructions.

Frontal cortex and hippocampus AChE estimation

Acetylcholinesterase (AChE) enzyme estimation was performed using the method described by **(Ellman, Courtney, Andres, & Featherstone, 1961)**. Animals were decapitated, and their brains were quickly removed and placed in ice-cold saline. The Frontal cortex and hippocampus were isolated, weighed, and homogenized in 0.1 M phosphate buffer (pH 8). A mixture containing 0.4 ml of homogenate, 2.6 ml of phosphate buffer (0.1 M, pH 8), and 100 µl of DTNB (10 mM) reagent was prepared. Then, 20 µl of acetylthiocholine iodide (0.075 M) solution was added. Absorbance was measured at 412 nm for 3 minutes, and the change in absorbance per minute was calculated. The rate of substrate hydrolysis per minute per gram of tissue was determined using the equation R = 5.74 × 10^−4 (ΔA/Co), where ΔA is the change in absorbance per minute, and Co is the original tissue concentration (mg/ml).

Western blott Analysis

Total protein from the uterus was extracted using RIPA lysis buffer supplemented with phosphatase and protease inhibitor cocktails. Equal amounts of protein (15 µg) were separated on 10% SDS-PAGE gels and then transferred onto polyvinylidene fluoride (PVDF) membranes. The membranes were blocked with 5% skim milk for 1 hour, followed by incubation with specific primary antibodies at a 1:1000 dilution overnight at 4°C. Mouse anti-β-actin (1:10000, Abcam) was used as a standard for protein quantification. Immunoreactive protein bands were detected using the Clarity Western ECL Substrate (Bio-Rad Laboratories).

Histopathological analysis

At the end of the treatment, all experimental animals were euthanized using the cervical dislocation method after 29 and 91 days. Following a 16-18 hour fasting period, the brain, kidney, liver, and heart were excised. Histopathological analysis was performed on brain sections (hippocampus and frontal cortex) by fixing them in formalin and overnight dehydration, followed by embedding in paraffin blocks. Slices of 4 µm were obtained from the paraffin blocks, and after deparaffinization, they were stained with hematoxylin and eosin dye. The Department of Pathology, IMS, B.H.U, Varanasi, conducted this work.

Statistical analysis

The results of the animal study were analyzed using mean ± SD (standard deviation). Intergroup comparisons of means were performed using one-way analysis of variance (ANOVA) test, followed by Dennett's multiple comparison tests for significantly different pairs. A probability value of $p<0.05$ was considered significant, and $p<0.001$ was considered highly significant. GraphPad Prism (version 8.0) was utilized for all statistical analyses. The Department of Biostatistics, IMS B.H.U. Varanasi, conducted the statistical analysis of the experimental results.

Results

*Dioscorea bulbifera*bioactive mining

Phytomolecules from *Dioscorea bulbifera* were systematically compiled by integrating bioactive information from the Traditional Chinese Medicine Systems Pharmacology Database and Analysis Platform (TCMSP), the Traditional Chinese Medicine Integrative Database (TCMID), and relevant literature reports. The compilation process involved storing the identified compounds in a standardized (.sdf) file format, and duplicates were meticulously removed to ensure data accuracy. A total of 44 unique compounds met the screening criteria and were identified in *Dioscorea bulbifera*. Each compound is represented by a distinct phytochemical identifier (PC) for ease of reference and analysis. As part of our screening process, we assessed the phytomolecules based on essential ADME parameters, including bioavailability (OB%) and druglikeness (DL). The table presents the ADME screening results, including blood-brain barrier permeability (BBBp) and Lipinski's Rule of 5 (RO5) compliance. The compounds' information was cross-validated through the PubChem database to further ensure reliability. This information has been summarized in Table 2.

Target prediction and disease association mining

The most crucial phase in mechanism prediction is target fishing. Each active substance that underwent screening has potential to interact with specific proteins based on their structural characteristics, offering protective effect against certain pathogenic processes. To identify potential targets or proteins for all active compounds, structures of each were submitted to online prediction systems/websites.

After removing duplicates, a total of 132 predicted targets (putative targets) were obtained and are listed in Table S1. Further analysis involved submitting the 132 putative targets to the DisGeNET server, resulting in the identification of 68 Direct Regulatory Targets (DRTs) associated with Alzheimer's disease, as presented in Table S3. These findings provide valuable insights into the potential therapeutic targets for the active compounds and their relevance to Alzheimer's disease.

Network construction and analysis

We utilized Cytoscape v3.7.1 to construct two bipartite networks from bioactive-target interaction data **(**Table S2) and target-disease association data (Table S3). Based on the network analysis, we observed varying degrees of interaction between the phytocompounds and their corresponding targets. Dioscorine (PC24) exhibited the highest degree of interaction with targets, having 20 degrees, closely followed by Diosbulbin B with 19 degrees. Phytocompounds 7-hydroxy-2,3,4-trimethoxyphenanthrene (PC42), 2,7-dihydroxy-3,4-dimethoxyphenanthrene (PC36), and stigmasterol (PC32) demonstrated 15 degrees of interaction with their targets. Additionally, seven compounds, namely Bafoudiosbulbin C (PC7), Bafoudiosbulbin F (PC8), Cyanidin (PC14), Dihydrodioscorine (PC16), Procyanidin B1 (PC28), 3,7-dihydroxy-2,4-dimethoxyphenanthrene (PC38), and 4-methoxyphenanthrene-2,3,7-triol (PC41), showed 13 degrees of interaction with their targets each. Based on degree of interaction, we ranked all compound accordingly (Table S4).

In the context of Alzheimer's disease, we identified a total of 52 genes associated with the condition. Additionally, five genes were associated with cognition disorders, three genes with dementia, two genes with impaired cognition, two genes with memory impairment, and four genes with neurodegeneration. Notably, certain genes such as CA2, CA12, OPRK1, and OPRM1 were modulated by ten phytocompounds, while CA7 and OPRD1 were influenced by nine phytocompounds, and MAOB was targeted by eight compounds. Furthermore, GSK3β, CA1, and BACE1 were found to be modulated by seven compounds, while ACHE was targeted by five compounds, and APP, ESR1, and ESR2 were influenced by four compounds.

Protein-Protein interaction mapping

Based on gene-disease association (GDA) scores, we identified 68 targets classified as direct regulatory targets (DRTs). Utilizing these DRTs, we constructed a protein-protein interaction network consisting of 68 nodes and 288 edges. The network analysis revealed an average node degree of 8.47 and an average local clustering coefficient of 0.5. Moreover, the PPi enrichment P-value was found to be < 1.0e-16, indicating the biological relevance of the network (as depicted in Figure 2). The protein-protein interaction network was imported from the String database to the Cytoscape software, allowing for further analysis to select the potential regulatory targets (PRTs). These PRTs represent the core network of genes modulated by *Dioscorea bulbifera* (DB) in the context of Alzheimer's disease treatment.

Table 2: List of Bioactive compounds identified in *Dioscorea bulbifera*

SN	PC ID	PhytocompoundName	PubChem ID	OB%	DL	BBBp	Lipinski'sRO5	Source	Target
1.	PC18	Diosbulbin B	9974762	43.01	0.70	0.46	Yes.	Kumar et al. 2017	18
2.	PC24	Dioscorine	442635	55.00	0.77	0.48	Yes.	Kumar et al. 2017	16
3.	PC32	Stigmasterol	5280794	48.83	0.76	1.00	Yes.	Adeniran and Sonibare 2018	15
4.	PC44	Jaranol	5318869	50.83	0.29	-0.22	Yes	Screened	15
5.	PC7	Bafoudiosbulbin C	101434898	55.00	0.04	0.31	Yes.	Screened	14
6.	PC27	Myricetin	5281672	13.75	0.31	-1.01	Yes.	Ghosh et al. 2013	14
7.	PC36	2,7-dihydroxy-3,4-dimethoxyphenanthrene	158975	55.00	0.10	0.39	Yes.	Screened	14
8.	PC37	2′, 3-dihydroxy- 5-methoxybibenzyl	91542987	55.00	0.52	0.36	Yes.	Screened	14
9.	PC42	7-hydroxy-2, 3, 4-trimethoxyphenanthrene	11997529	55.00	0.10	0.44	Yes.	Screened	14
10.	PC1	2,4,3,5′-Tetrahydroxybibenzyl	16126762	55.00	0.09	0.32	Yes.	Screened	13
11.	PC5	Bafoudiosbulbin A	101410701	55.00	0.44	0.25	Yes.	Le et al. 2006	13
12.	PC8	Bafoudiosbulbin F	102479350	55.00	0.29	0.43	Yes.	Screened	13
13.	PC14	Cyanidin	128861	55.00	0.58	0.28	Yes.	Kumar et al. 2017	13
14.	PC20	Diosbulbin D	100021	55.00	0.29	0.43	Yes.	Screened	13
15.	PC28	Procyanidin B1	11250133	67.87	0.66	-1.97	No.	Screened	13
16.	PC29	Quercetin-3-O-Beta-D-galactopyranoside	5280804	1.86	0.77	-2.31	No.	Padhan and Panda 2020	13
17.	PC38	3, 7-dihydroxy-2, 4-dimethoxyphenanthrene	10445823	80.73	0.24	0.35	Yes.	Screened	13
18.	PC41	4-methoxyphenanthrene-2, 3, 7-triol	5319480	55.00	0.71	0.34	Yes,	Screened	13

19. PC2	2,4,6,7- Tetrahydroxy-9,10-dihydrophenanthrene	22753774	24.36	0.19	0.02	Yes.	Screened	12
20. PC39	3′, 3′-dihydroxy- 5-methoxybibenzyl	67233527	55.00	0.14	0.23	Yes.	Screened	12
21. PC9	Bafoudiosbulbin G	102479351	55.00	0.29	0.42	Yes.	Screened	11
22. PC10	Caryatin	5489501	17.79	0.33	-0.27	Yes.	Screened	11
23. PC15	Demethylbatatasin IV	442699	69.74	0.11	0.30	Yes.	Screened	11
24. PC25	Diosgenin	99474	80.88	0.81	0.27	Yes	Ghosh et al. 2013; Kumar et al. 2017; Padhan and Panda 2020	11
25. PC26	kaempferol	5280863	41.88	0.24	-0.55	Yes.	Adeniran and Sonibare 2018	11
26. PC43	latifolin	340211	55.00	0.24	0.43	Yes.	Screened	11
27. PC21	Diosbulbin F	181851	22.37	0.55	-0.87	Yes.	Screened	10
28. PC22	Diosbulbin G	329252	55.00	0.52	0.28	Yes.	Screened	10
29. PC30	Sapogenin	4483642	56.00	0.20	1.83	Yes.	Kumar et al. 2017 Padhan and Panda 2020	10
30. PC33	Tannin	44144428	11.00	0.10	0.00	No.	Ghosh et al. 2013; Kumar et al. 2017; Padhan and Panda 2020	10
31. PC40	4, 7-dihydroxy-2-methoxy-9, 10-dihydrophenanthrene	133612121	17.00	0.10	0.00	No.	Screened	10
32. PC16	Dihydrodioscorine	15931602	55.00	0.70	0.47	Yes.	Literature: Kumar et al. 2017	9
33. PC31	Saponin	198016	17.00	0.24	0.34	No.	Literature: Kumar et al. 2017 Padhan and Panda 2020	9
34. PC3	5,7,4′-Trihydroxy-2-styrylchromone	129834558	55.00	0.43	0.31	Yes.	Screened	8
35. PC19	Diosbulbin C	15559045	56.00	0.05	0.26	Yes.	Screened	7
36. PC4	Allantoin	204	55.00	0.88	0.17	Yes.	Literature: Padhan and Panda 2020	6
37. PC23	Dioscin	119245	17.75	0.06	-3.05	No.	Literature: Padhan and Panda 2020	6
38. PC11	Catechin	9064	54.83	0.24	-0.73	Yes.	Literature: Ghosh et al. 2013	1
39. PC34	β-sitosterol	521199	55.00	0.11	0.40	Yes.	Literature: Adeniran and Sonibare 2018	1
40. PC6	Bafoudiosbulbin B	102479349	55.00	0.11	0.24	Yes.	Literature: Le et al. 2006	0
41. PC12	Chrysanthemin	197081	17.00	0.06	1.61	No.	Screened	0
42. PC13	Cortisone	222786	55.00	0.15	0.22	Yes.	Literature: Padhan and Panda 2020	0
43. PC17	Diosbulbin A	177106	55.00	0.22	0.26	Yes.	Literature: Kumar et al. 2017	0
44. PC35	2-7-dihydroxy-4-methoxy phenanthrene	312247658	-	-	-	-	Screened	0

Gene Ontology enrichment analysis of direct regulatory targets (DRTs)

Through comprehensive GO enrichment analysis, we meticulously annotated all the Direct Regulatory Targets (DRTs) for their involvement in three critical aspects: cellular component, biological process, and molecular function. The analysis revealed highly significant enrichment in each category, uncovering key functional characteristics of the DRTs. In terms of cellular component, the most remarkably enriched term was "nicotinic acetylcholine-gated receptor-channel complex," with an impressive gene fold of 77.9. This finding suggests a strong association between the DRTs and cellular components related to nicotinic acetylcholine receptors and their associated channel complexes.

Regarding biological processes, the DRTs exhibited extraordinary enrichment in "neurotransmitter metabolism," boasting a substantial gene fold of 133.9. This observation highlights the critical involvement of these targets in biological processes essential for neurotransmitter metabolism, possibly indicating their significance in modulating neurotransmission. Furthermore, the molecular function analysis revealed a striking enrichment in "Aspartic-type signal peptidase activity," with an impressive gene fold of 38.4. This suggests a pivotal role of the DRTs in molecular functions associated with aspartic-type signal peptidases, crucial players in protein processing and secretion. The GO enrichment analysis unraveled a wealth of functional insights, shedding light on the intricate roles of the DRTs in various cellular processes.

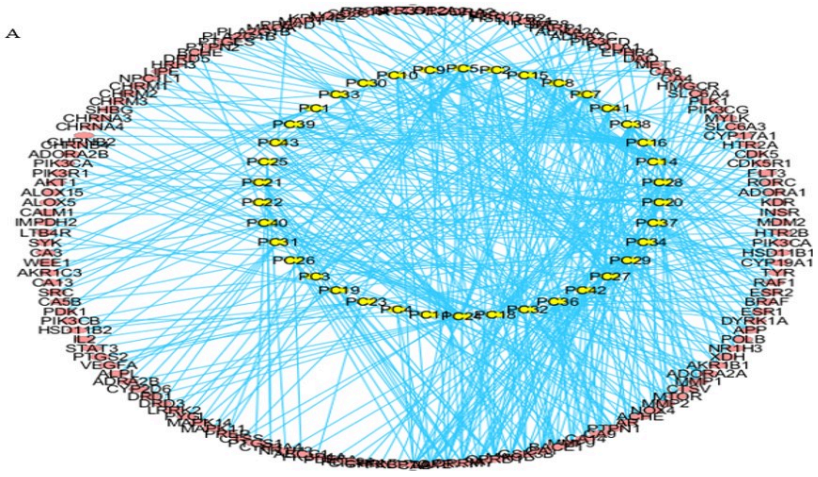
These findings provide a comprehensive understanding of the biological mechanisms and pathways influenced by these regulatory targets. (Figure 3 showcases the visualization of the enrichment analysis results, providing a graphical representation of the significant findings.)

Screening of Potential Regulatory Targets (PRTs) for AD Treatment

The identification of potential regulatory targets (PRTs) for *Dioscorea bulbifera* (DB) in treatment of Alzheimer's Disease (AD) involved a comprehensive approach. Firstly, top modulated targets interacting with DB's bioactive compounds were ranked based on degree topological parameter. Simultaneously, targets associated with AD were ranked using gene-disease association score (DRTs). Additionally, top targets modulated by protein-protein interactions, mapped by network parameter-degree distribution, were included in analysis. Through this integrative analysis, a total of fifteen genes emerged as PRTs, representing intersection of putative DB targets with AD-related genes. These fifteen genes exhibit potential as crucial regulatory targets of DB in context of AD treatment. Since proteins rarely function in isolation, protein-protein interactions (PPIs) play a crucial role in predicting target protein function and drug-like properties of compounds. Considering this significance, top 10 genes based on PPi were also included in list of PRTs (Table 3). By combining multiple layers of information, including bioactive interactions, disease asso-ciations, and protein-protein interactions, we have identified a select group of genes that hold promise as potential targets for DB in treatment of AD. These findings provide valuable foundation for further investigations % potential therapeutic strategies for AD. (Figure 4 visually represents integration of information, While Table 3 presents a concise list of the top potential regulatory targets.)

Pathway enrichment analysis of potential regulatory targets (PRTs)

Gene's involvement in important signaling pathways can be identified through pathway-enrichment analysis. The potential regulatory targets (PRTs) were used to predict top ten enriched pathways modulated by them as shown in Figure 5 and Table 4. Neurotransmitter clearance in synaptic cleft, melatonin degradation II, monoamines are oxidized to aldehyde by MAOA and MAOB producing NH3 and H2O2, AP-1 transcription factor network, dopamine clearance from synaptic cleft, integrin-linked kinase signaling pathways, amine oxidase reactions, 3-phosphoinositide biosynthesis, phenylalanine degradation IV and super pathway of melatonin degradation were all significantly enriched. Acetylcholine is one of most well-known neurotransmitters associated with AD. Dysfunction in neurotransmission is primarily caused by toxic buildup of A plaques in neurons, which causes neuronal degeneration. The neuroanatomy of monoaminergic systems, such as serotonergic and dopaminergic system, is impaired in AD patients (Roy et al. 2021). Acetylcholine clearance in synaptic cleft is tightly regulated by acetylcholinesterase (AChE) enzyme, Disturbances in levels of (AChE) may contribute to neurodegenerative diseases as well as depressive disorders (Walczak-nowicka and Herbet 2021). Based on this network pharmacological analysis, it is hypothesized that DB treatment of AD is by regulation of acetylcholine clearance & measuring cellular acetylcholine concentration can validate mechanism. Concentration of acetylcholine also highly corelates with intrinsic estrogen levels (Mitsushima et al. 2009), hence the concentration of estrogen was also investigated.



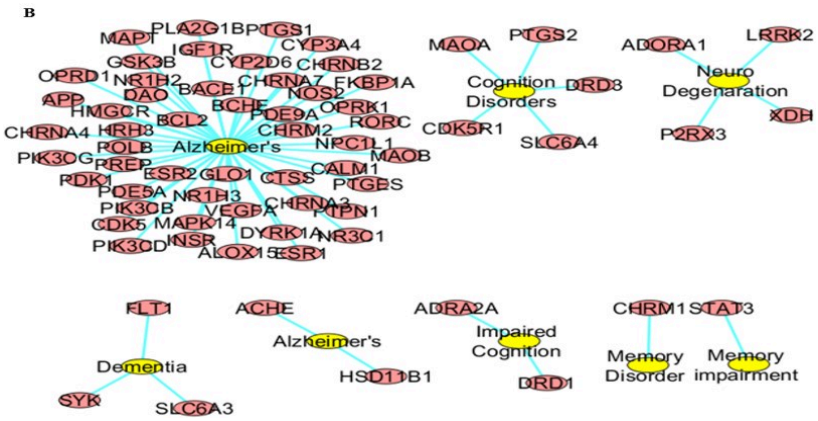


Figure 1: Pharmacological network showing **A)** Bioactive-Target association, where the outer layer represents predicted targets, and the inner layer represents phytochemicals. **B)** An association network between genes and AD related conditions.

Verification of the interaction between bioactive and target genes

Through in-depth analysis, we identified most important pathway related to treatment of Alzheimer's Disease (AD) as "neurotransmitter clearance in synaptic cleft signaling." In this context, six core target genes enriched in pathway were chosen for further investigation: ESR1, APP, GSK3B, BACE1, AChE, and MAOB.

To explore binding interactions between these target genes and specific compounds, we conducted molecular docking using dedicated software. The results, which are presented in Table 5, revealed interesting findings for various compounds interacting with target genes. Myricetin, for instance, exhibited most favorable binding energy of -13.410. It formed two Pi-Pi stacking interactions with TRP286 and TYR341, and an additional hydrogen bond with PHE295 in binding site of acetylcholinesterase (AChE).

Moreover, Myricetin showed a binding energy of -10.63, interacting with ARG235, ASH32, GLY34, THR72, THR231, and THR232 through hydrogen bonds in binding site of BACE1 (Figure 6 (A)). Similarly, Tannin demonstrated strong interactions with the target genes. It exhibited a binding energy of -12.433 and formed hydrogen bonds with ARG235, GLY34, LYS224, SER328, THR72, and THR231 in the binding site of BACE1.

Additionally, Tannin showed a binding energy of -11.358, engaging in hydrogen bonding with VAL340 and forming hydrogen bonds with ARG296, ASP74, GLU292, SER292, TYR77, as well as Pi-Pi stacking with TRP286 in the binding site of AChE (Figure 6 (A)).

Caryatin displayed a binding energy of -7.632 and interacted with ARG235, GLY34, PHE108, THR72, and THR231 through hydrogen bonds in the binding site of BACE1. Furthermore, it showed a binding energy of -3.83, forming hydrogen bonds with ALA16, CYS14, and engaging in Pi-Pi stacking with Phe34 in the binding site of APP (Figure 6 (B)). Additionally, Demethylbatatasin IV exhibited a binding energy of -9.162, forming hydrogen bonds with ARG394, GLU353, and LEU346, as well as Pi-Pi stacking with PHE404 in the binding site of Estrogen receptor alpha (ESR1).

Moreover, it displayed a binding energy of -8.798, engaging in Pi-Pi stacking with TYR326 in the binding site of MAOB, and a binding energy of -6.863, forming hydrogen bonds with PRO136 and VAL135 in the binding site of GSK3B (Figure 6 (C)). Another compound, 2,4,3,5'-Tetrahydroxybibenzyl, exhibited a binding energy of -9.258, interacting with GLU353, HIE524, LEU387 through hydrogen bonds, and engaging in Pi-Pi stacking with PHE404 in the binding site of ESR1. Additionally, it showed a binding energy of -6.714, forming hydrogen bonds with PRO136 and VAL135 in binding site of GSK3B, and a binding energy of -3.261, interacting with ALA9 and PHE34 through hydrogen bonds, and also engaging in Pi-Pi stacking with PHE34 (Figure 6 (D)). Furthermore, 2,4,6,7-Tetrahydroxy-9,10-dihydrophenanthrene displayed a binding energy of -7.166, interacting with TYR134 and Val135 through hydrogen bonds. Latifolin showed a binding energy of -7.099, engaging in a hydrogen bond with VAL135. Lastly, β-sitosterol demonstrated a binding energy of -3.996, interacting with LYS183 through hydrogen bonding. All these interactions occurred in the binding site of GSK3B.

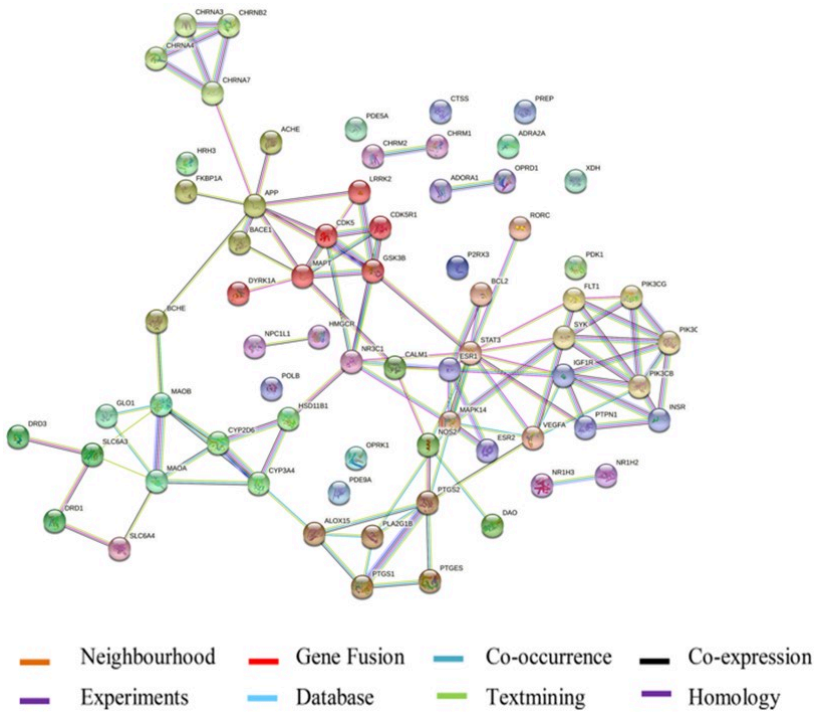


Figure 2: Protein-Protein interaction network of DB in Alzheimer's Disease (AD) with 68 direct regulatory targets (DRTs) as seeds.

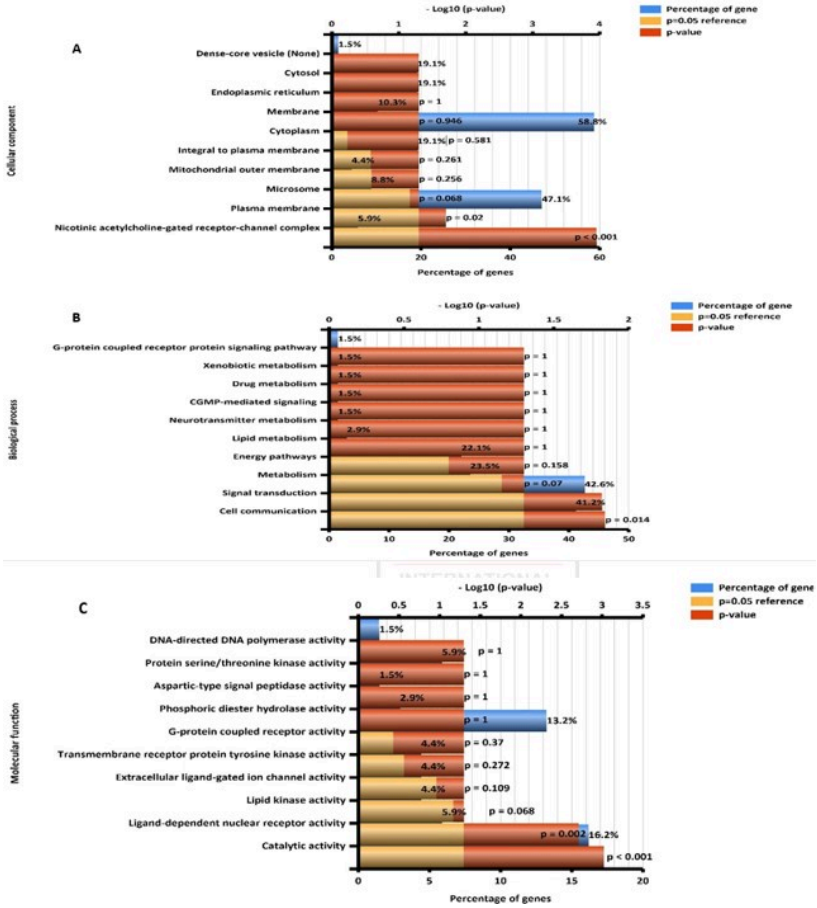


Figure 3: Gene Ontology (GO) enrichment analysis of AD modulating genes with top 10 enriched terms **A)** Cellular component. **B)** Biological process. **C)** Molecular function. The most significantly enriched terms for these three categories are nicotinic acetylcholine-gated receptor-channel complex as a cellular component with a gene fold of 77.9, neurotransmitter metabolism as a biological process with a 133.9 gene fold, and Aspartic-type signal peptidase activity molecular function with 38.4 gene fold.

Moreover, Quercetin-3-O-Beta-D-galactopyranoside displayed a binding energy of -7.708, forming hydrogen bonds with HIE287, SER293, and TYR72, and engaging in Pi-Pi stacking with TRP286 in the binding site of AChE. Additionally, 7-hydroxy-2,3,4-trimethoxyphenanthrene exhibited a binding energy of -8.984, forming two Pi-Pi stacking bonds with TRY326 in the binding site of MAOB, and a binding energy of -5.837, interacting with VAL135 via a hydrogen bond in the binding site of GSK3B. Bafoudiosbulbin A displayed a binding energy of -2.888, forming hydrogen bonds with LYS60 and TYR134 in the binding site of GSK3B. Furthermore, it showed a binding energy of -2.820, interacting with ARG235 and THR232 through hydrogen bonds in the binding site of BACE1. Finally, Stigmasterol (binding energy -5.542) and Diosgenin (binding energy 1.370) exhibited weaker interactions with AChE & APP, respectively. Data from these interactions, along with a standard compound Donepezil, Has been summarized in Table 5, providing comprehensive overview of binding energies and specific interactions of each compound with target genes.

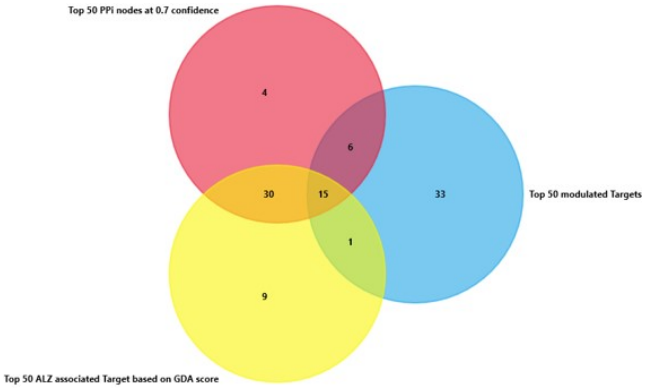


Figure 4: The intersection of the top 50 targets modulated by DB bioactive, the top 50 AD targets associated with GDA scores (DRTs), and the top 50 targets modulated by protein-protein interactions at 0.7 confidence.

Table 3: Shared genes of putative DB targets and AD-related genes: (PRTs)

SN	Gene	No. of interacting phytocompounds	PhytocompoundID's	GDA Score	Degree ofPPi
1.	ESR1	4	PC1 PC15 PC32 PC37	0.944	7
2.	APP	4	PC1 PC10 PC25 PC37	0.900	9
3.	GSK3B	7	PC1 PC2 PC5 PC15 PC34 PC42 PC43	0.700	7
4.	MAPT	2	PC14 PC27	0.700	8
5.	BACE1	7	PC5 PC7 PC9 PC10 PC27 PC33 PC39	0.600	2
6.	IGF1R	3	PC1 PC14 PC37	0.560	7
7.	ACHE	5	PC27 PC29 PC32 PC33 PC40	0.400	1
8.	MAOB	8	PC15 PC16 PC24 PC33 PC36 PC38 PC41 PC42	0.400	6
9.	VEGFA	2	PC23 PC28	0.400	6
10.	SLC6A3	3	PC18 PC20 PC16	0.360	4
11.	PTGS2	2	PC4 PC29	0.330	7
12.	CDK5R1	3	PC15 PC36 PC42	0.320	4
13.	STAT3	2	PC23 PC40	0.310	13
14.	MAOA	2	PC14 PC33	0.310	6
15.	SLC6A4	3	PC18 PC20 PC32	0.300	2
16.	ADORA1	3	PC18 PC25 PC10	0.300	1
17.	MAPK14	2	PC5 PC7	0.300	7
18.	DYRK1A	4	PC38 PC36 PC37 PC39	0.100	1
19.	PIK3CG	3	PC18 PC27 PC43	0.100	4
20.	NR3C1	4	PC7 PC8 PC21 PC22	0.100	7
21.	PIK3CB	2	PC3 PC18	0.100	7
22.	PIK3CD	3	PC3 PC18 PC43	0.100	6
23.	DAO	3	PC3 PC4 PC15	0.040	1
24.	OPRD1	9	PC5 PC7 PC8 PC9 PC18 PC19 PC20 PC21 PC22	0.030	1
25.	NR1H3	4	PC14 PC25 PC32 PC34	0.020	1

Table 4: Top ten enriched pathways modulated by DB

SN	Biological pathway	Percentage	log10(P-value)	Fold
1.	Neurotransmitter clearance in the synaptic cleft	13%	2.85	136.9
2.	Melatonin degradation II	8.7%	1.67	273.4
3.	Monoamines are oxidized to aldehyde by MAOA and MAOB producing NH3 and H2O2	8.7%	1.67	273.4
4.	AP-1 transcription factor network	43.5%	1.32	4.4
5.	Dopamine clearance from the synaptic cleft	8.7%	1.19	182.5
6.	Integrin-linked kinase signaling pathways	43.5%	1.13	4.2
7.	Amine oxidase reaction	8.7%	0.89	137
8.	3-phosphoinositide biosynthesis	13%	0.76	31.6
9.	Phenylalanine degradation IV	8.7%	0.67	109.7
10.	Superpathway of melatonin degradation	8.7%	0.67	109.7

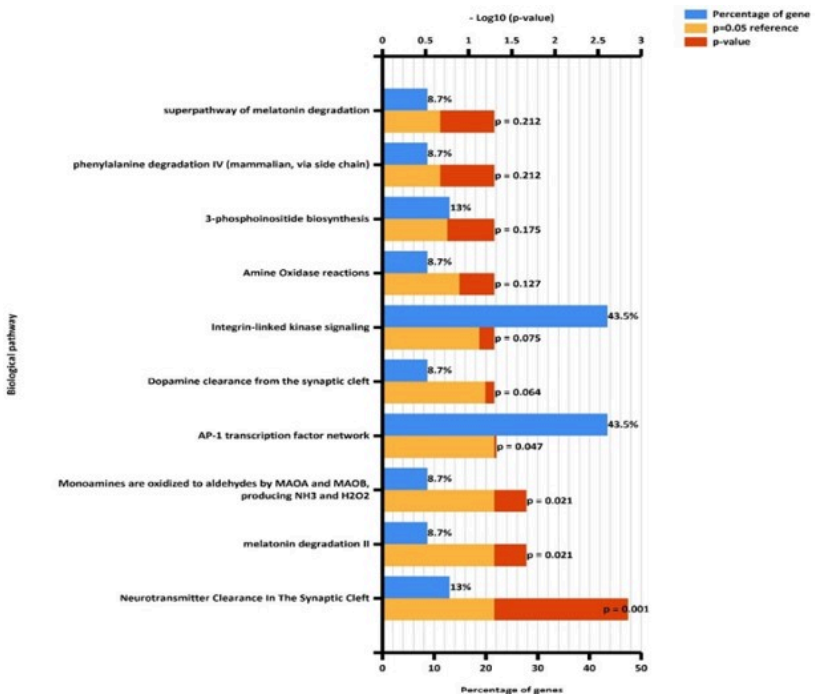


Figure 5: The top-ten enriched pathways modulated by the potential regulatory targets. Neurotransmitter clearance in the synaptic cleft, melatonin degradation II, monoamines are oxidized to aldehyde by MAOA and MAOB producing NH3 and H2O2, AP-1 transcription factor network, dopamine clearance from the synaptic cleft, integrin-linked kinase signaling pathways, amine oxidase reactions, 3-phosphoinositide biosynthesis, phenylalanine degradation IV and super pathway of melatonin degradation were all significantly enriched.

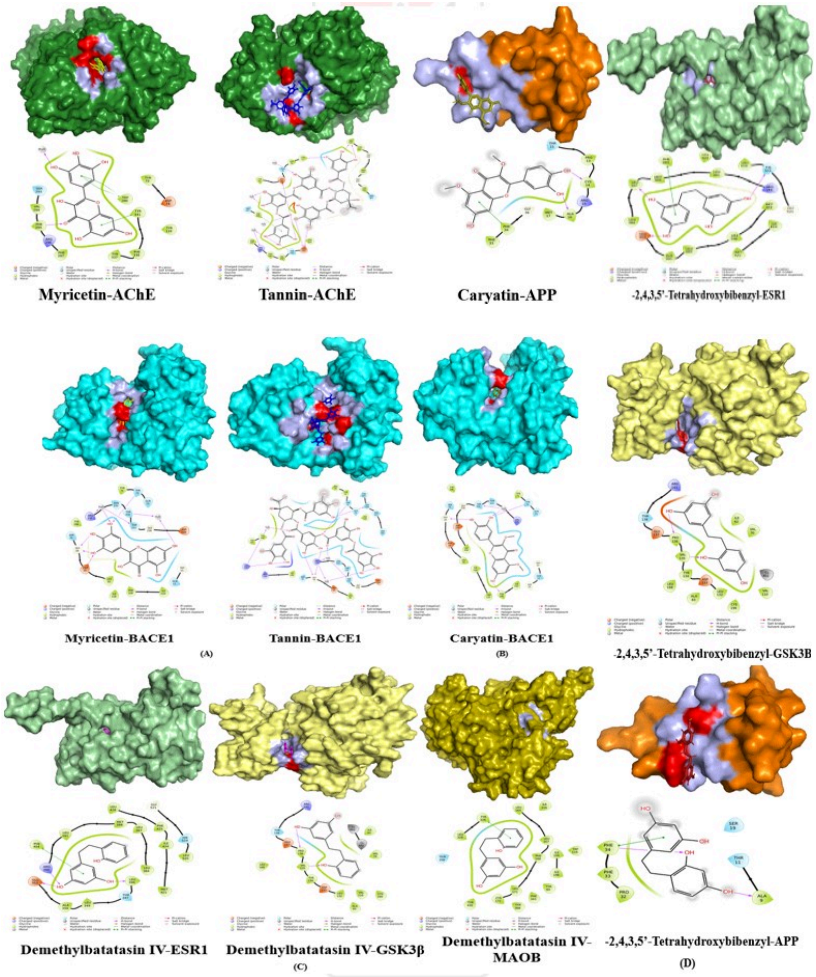


Figure 6: Molecular docking of core target genes and bioactive. **A)** Docking concept and binding site analysis of Myricetin and Tannin. **B)** Docking concept and binding site analysis of Caryatin. **C)** Docking concept and binding site analysis of Demethylbatatasin IV. **D)** Docking concept and binding site analysis 2,4,3,5'-Tetrahydroxybibenzyl

Table 5: Docking score of core genes (interacting amino acid). Bold signifies the maximum score of active components

Bioactive	AChE (PDB ID: 4M0E)	ESR1 (PDB ID: 1A52)	GSK3B (PDB ID: 7OY5)	MAOB (PDB ID: 6FWC)	BACE1 (PDB ID: 6NV7)	APP (PDB ID: 1AAP)
Myricetin	-13.410 (TRP286-Pi-Pi stacking, TYR341-Pi-Pi stacking, PHE295-H bond)				-10.63 (THR72-Hbond, THR 232-Hbond, THR 231-Hbond, ASH32-Hbond, GLY34-2Hbond, ARG235-Hbond)	
Tannin	-11.358 (VAL340-2Hbonds, TYR77-Hbond, ASP74-Hbond, GLU292-2Hbonds, SER293-Hbond, ARG296-Hbond, TRP286-Pi-Pi stacking)				-12.433 (THR72-Hbond, SER 328-Hbond, THR231-Hbond, ARG235-Hbond, GLY34-2 Hbond, LYS224-Hbond)	
Donepezil (Reference)	-8.231 (PHE294-Hbond, TRP285-Pi-Pi stacking)					
Quercetin-3-O-Beta-D-galactopyranoside	-7.708 (TYR72-Hbond, SER293-Hbond, TRP286-Pi-Pi stacking, HIE287-Hbond)					
Demethylbatatasin IV		-9.162 (LEU346-Hbond, ARG394-Hbond, Glu353-Hbond, PHE404-Pi-Pi stacking)	-6.863 (VAL135-Hbond, PRO136-Hbond)	-8.798 (TYR326-Pi-Pi stacking)		
2,4,6,7- Tetrahydroxy-9,10-dihydrophenanthrene			-7.166 (TYR134-Hbond, VAL135-Hbond)			
latifolin			-7.099 (VAL135-Hbond)			
β-sitosterol			-3.996 (LYS183-Hbond)			
Stigmasterol	-5.542					
Caryatin					-7.632 (THR231-Hbond, THR72-Hbond, ARG235-Hbond, PHE108-Hbond, GLY34-Hbond)	-3.83 (CYS14-Hbond, ALA16-Hbond, Phe34-Pi-Pi stacking)
-2,4,3,5'-Tetrahydroxybibenzyl		-9.258 (HIE524-Hbond, GLU353-Hbond, LEU387-Hbond, PHE 404-Pi-Pi stacking)	-6.714 (VAL135-Hbond, PRO136-Hbond)			-3.261 (ALA9-Hbond, PHE34-Hbond, PHE34-Pi-Pi stacking)
7-hydroxy-2, 3, 4-trimethoxyphenanthrene			-5.837 (VAL135-Hbond)	-8.984 (TYR326-2 Pi-Pi stacking)		
Bafoudiosbulbin A			-2.888 (TYR134-Hbond, LYS60-Hbond)		-2.820 (THR232-Hbond, ARG235-Hbond)	
2', 3-dihydroxy- 5-methoxybibenzyl						-3.429
Diosgenin						1.370

Animal Experimentation

Elevated plus maze (EPM) test

Transfer latencies were notably higher in the scopolamine-treated rats compared to all other groups (P<0.001) during both the acquisition (day 28) and retention (day 29) sessions **(Figure 7a)**. Conversely, rats treated with scopolamine and 200 mg of *DB* extract exhibited lower transfer latencies, similar to the Control Group (P>0.05), during both trial sessions. Notably, the lowest transfer latencies were observed in the group treated with 400 mg of *DB* extract (Group V). Additionally, no significant differences in transfer latencies were observed between the Control Group and Groups III, IV, and VI (P>0.05) during both the acquisition and retention trial sessions.

The Morris water maze test (MWM)

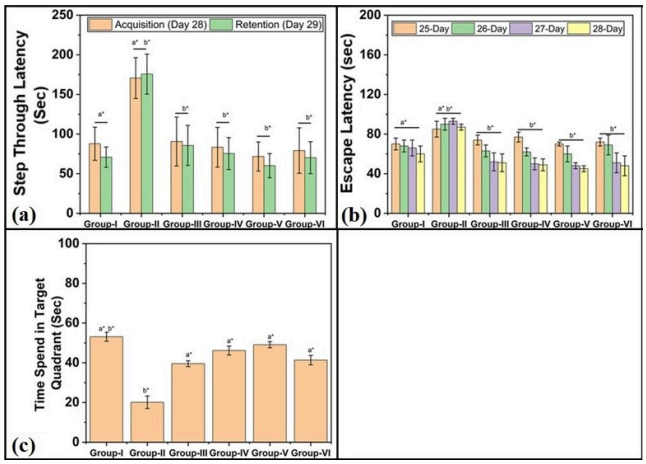


Figure 7: Effect of *DB* on memory impairment using **a)** Elevated Plus Maze **b)** Morris Water Maze **c)** Probe trial session (MWM) paradigm. The findings of each experiment were carried out in triplicate and they are presented as mean ± standard deviation (SD). The statistical evaluation of the data was performed using t test with a significance a*P<0.05 and b*P<0.001.

The acquisition sessions (days 25-28) revealed that scopolamine-treated group (Group II) exhibited significantly longer escape latencies compared to OVX control group (P<0.05), an effect alleviated by co-administration of *DB* extract **(Figure 7b)**. Significant reductions in escape latencies were noted on days 2-4 (treatment days 26-28) compared to day 1 (treatment day 25) in OVX control group, but these improvements were absent in scopolamine-treated rats. Notably, co-administration of scopolamine with *DB* extract (200 mg, 400 mg, and 800 mg) restored escape latencies.

Additionally, Group III (estradiol 20 µg/kg bw/day & Donepezil 3mg/kgbw) exhibited decreased escape latencies during the acquisition sessions (P<0.001). On the probe trial session day (day 29), scopolamine-treated rats spent significantly more time searching the target quadrant compared to the controls (P<0.001). Conversely, rats co-administered with the *DB* extract (Groups IV, V, VI) and those in Group III spent less time in the target quadrant compared to Group I (**Figure 7c)** (P<0.05**)**, suggesting that low estradiol levels are responsible for memory impairment in the young postmenopausal (OVX) animal model.

Effect of *DB* on E2, Insulin, AChE and ER-α

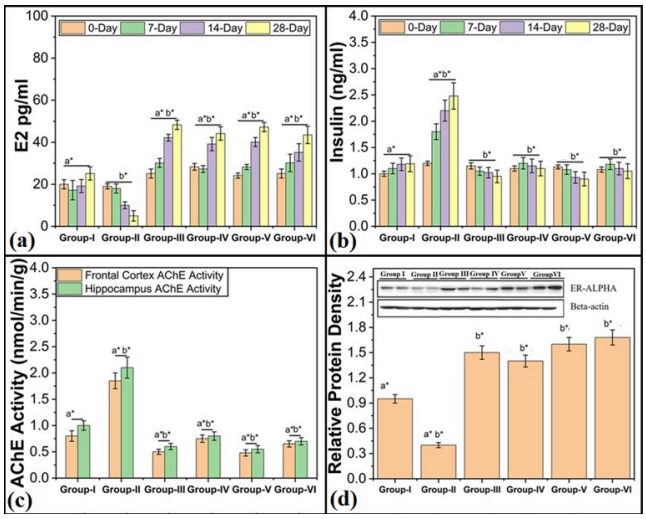


Figure 8: A) Effect of hydro-alcoholic tubers extract of*Dioscorea bulbifera*at 200, 400, and 800 mg/kg BW/day activity in the regulation of estradiol 20 µg/kg BW/day levels in cognitively impaired rats. **B)** Effect of hydro-alcoholic tubers extract of*Dioscorea bulbifera*(at 200, 400, and 800 mg/kg BW/day) and estradiol (20 µg/kg BW/day) on acetylcholine level in the different regions of the brain (Frontal cortex & Hippocampus) of scopolamine treated rats.

Scopolamine-treated rats exhibit a significant decrease in 17-β estradiol (E2) levels compared to OVX normal-treated rats. *DB* extract, administered at doses of 200, 400, and 800 mg/kg body weight per day, along with estradiol valerate injections at 20 µg/kg body weight per day and Donepezil (3 mg/kg/day) for 28 days, significantly increased E2 levels in groups III, IV, V, and VI compared to group I (P<0.05) and with Group II (P<0.001), with the 400 mg/kg dose showing notable improvement (**Figure 8a**). Insulin resistance was highest in scopolamine-treated rats (Group II) and significantly reduced in treated groups,

With Group III, Group IV, Group V and Group VI showing comparable reductions (P<0.001) (**Figure 8b**). AChE activity was highest in Group II and significantly lowered in treated groups (P<0.001), with Group V showing slightly better AChE inhibitory activity compared to Group III (**Figure 8c**). ER-α protein density was lowest in Group II and increased in treated groups (P<0.001), with the highest levels in Group VI (**Figure 8d**)**.** Overall, *DB* extract and standard treatments effectively improved E2 levels, reduced insulin resistance, decreased AChE activity, and increased ER-α protein density in a dose-dependent manner.

Histopathological Evaluation

Histopathological examinations were conducted to assess the condition of nerve cells in the brain's frontal cortex and hippocampus. Notably, the Ovx+ scopolamine (2 mg/kg BW/day; IP) treated Group II exhibited noticeable damage to nerve cells in these brain regions when compared to the OVX control group. However, encouragingly, the damage observed in the scopolamine-treated group was significantly reduced when treated with *Dioscorea bulbifera* hydro-alcoholic tubers extract, as depicted in **Figure 9**. This indicates the potential neuroprotective effects of the DB extract in mitigating the damage caused by scopolamine and suggests its possible role in preserving nerve cell integrity in the frontal cortex and hippocampus.

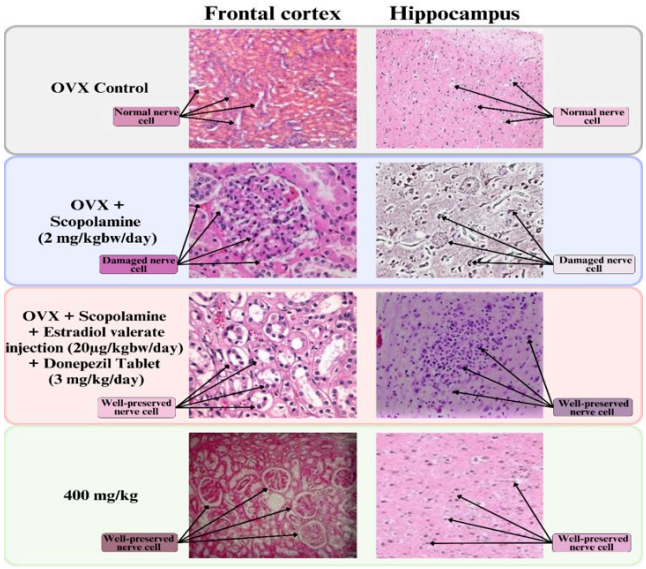


Figure 9: DB has a neuroprotective effect on Scopolamine induced frontal cortex and Hippocampus neuronal damage. Histopathological analysis of rat brain tissue from the frontal cortex and hippocampus at 40x magnification.

Discussion

In this study, we conducted an extensive investigation into the active ingredients and potential targets of *Dioscorea bulbifera* for the treatment of Alzheimer's disease (AD) using an integrative network pharmacology approach. Through the combination of TCMSP, TCMID, and literature mining, we identified 44 active compounds that met specific criteria (OB ≥ 30%, DL ≥ 0.18, and BBBp ≥ -0.3). Using 'Swiss Target Prediction' and 'BindingDB' databases, we predicted 132 targets associated with these compounds. To further refine the targets, the 'DisGeNET' server was employed, resulting in 68 genes identified as direct regulatory targets (DRTs) associated with AD.

Building on this, we utilized the DRTs as seeds to construct a protein-protein interaction network using 'STRING.' The resulting network consisted of 68 nodes and 288 edges, with an average node degree of 8.47 and an average local clustering coefficient of 0.5. The significant PPI enrichment (P-value < 1.0e-16) further validated the relevance of the interactions. To identify the top twenty-five AD-related genes, we employed three criteria: the number of interacting phytocompounds, the gene-disease association (GDA) score, and the degree of protein-protein interaction (PPI). These selected genes were defined as potential regulatory targets (PRTs) for *Dioscorea bulbifera* in AD treatment. Next, we conducted GO and pathway enrichment analysis on the PRTs. The results revealed cellular component terms, such as nicotinic acetylcholine-gated receptor channel complex; biological process terms, including cell communication; and molecular function terms, particularly ligand-dependent nuclear receptor activity, to be significantly enriched. Additionally, the top enriched pathway was related to neurotransmitter clearance in the synaptic cleft signaling.

For a more in-depth analysis of network pharmacology, we performed molecular docking of active compounds with six core targets associated with neurotransmitter clearance in the synaptic cleft signaling, namely ESR1, APP, GSK3β, BACE1, AChE, and MAOB. This analysis provided valuable insights into the interactions and potential mechanisms of action. It is worth noting that each of these core genes represents a key biomarker of AD pathogenesis, suggesting their importance in the potential therapeutic effects of *Dioscorea bulbifera*.

These findings contribute to a better understanding of the molecular interactions involved and pave the way for future research and development of *Dioscorea bulbifera* as a potential treatment option for Alzheimer's disease. The core genes implicated in Alzheimer's disease (AD) demonstrate a high level of interplay and cross-talk, working together in synergy to drive disease progression. One significant factor influencing AD's prevalence in women could be the decline in estrogen levels post-menopause. Estrogens exert their effects through binding to estrogen receptors (ER), influencing mRNA levels, protein production, and physiological responses (Deroo and Korach, 2006).

Notably, ER has been found to interact closely with tau proteins in AD brains, leading to increased ER-tau interactions. This interaction results in tau overexpression, which inhibits ER transcriptional activity and co-localizes with tau hyperphosphorylation in neurofibrillary tangles (Wang et al., 2016). Moreover, the transcriptomic profile of genes regulated by estradiol-ESR1 indicates a direct relationship between APP (Amyloid Precursor Protein) and ER (Cerny et al., 2016). Aβ (APP) is a target of estrogen action, affecting its synthesis, clearance, and degradation. Both Aβ and tau mutually interact in pathological signaling at the synaptic level (Merlo and Spampinato, 2017). Additionally, it has been observed that APP and tau can communicate with each other through specific peptide sections (Maron et al., 2020). In the context of impaired learning and memory in AD, several critical factors play roles, including GSK3β's involvement in tau hyperphosphorylation, increased Aβ generation from APP, and heightened microglial-mediated inflammatory responses (Simone et al., 2021). The pathogenesis of AD, which includes amyloid peptide (A) synthesis, neurofibrillary tangle formation, and cholinergic neuron death, is linked to the activation of monoamine oxidase (MAO) (Cai, 2014). The main cholinesterase in the body, acetylcholinesterase (AChE), plays a crucial role in AD. AChE's crosstalk with Aβ and P-tau modulates its activity, while the N-terminally extended T-AChE variant activates the tau kinase GSK-3β, causing tau hyperphosphorylation (Small, Avila, and Sáez-valero, 2011). Additionally, P-tau can boost AChE activity, and Aβ peptides can elevate AChE levels, influencing the pathways leading to amyloid formation and tau hyperphosphorylation (Small, Avila, and Sáez-valero, 2011).

Furthermore, AD is characterized by the loss of neurons expressing nicotinic acetylcholine receptors (nAChRs), resulting in decreased nAChR numbers (Buckingham et al., 2009). The complex interplay between these core genes highlights their role in AD pathogenesis and offers potential avenues for therapeutic interventions to combat this devastating neurodegenerative disease.

The results of this study demonstrate the potential of DB extract, containing compounds such as Myricetin, Demethylbatatasin IV, Latifolin, Tannin, Quercetin, Caryatin, Diosgenin, among others, in regulating the core targets implicated in AD, leading to symptom reversal. Particularly, DB extract primarily modulates the acetylcholine level by orchestrating cross-talk between the core genes, increasing intrinsic estrogen levels, and inhibiting acetylcholinesterase enzyme metabolism. The similarity in targets and pathways modulated by estrogen and DB suggests that DB might exhibit estrogen-like activity, which was further supported by in vivo studies using OVX rats.

In these experiments, DB extract at a dose of 400 mg/kg BW/day effectively reversed scopolamine-induced memory impairment, as evidenced by Morris water maze and elevated plus maze tests. ELISA analysis confirmed a dose-dependent increase in acetylcholine and estrogen concentrations following DB treatment. The neuroprotective effects of DB were also evident in histopathological analysis using H&E staining, possibly attributed to the targeting of the nicotinic acetylcholine receptor signaling pathway, as predicted by GO enrichment analysis.

Notably, the effects of DB extract at the 400 mg/kg BW/day dose were found to be comparable, if not superior, to those of an estrogen analog in improving AD symptoms. This suggests that DB extract, with its combination of compounds, could serve as a promising adjunct therapy alongside standard treatments for AD, without the associated side effects of estrogen-based therapies.

By regulating the predicted biomarkers and pathways, DB extract shows great potential in mitigating the progression of AD. Nevertheless, further investigations and clinical studies are warranted to validate and corroborate these findings, paving the way for the development of DB extract as a safe and effective therapeutic option for AD patients.

Conclusion

Our study presents a novel and comprehensive approach utilizing integrated network pharmacology and artificial intelligence to unravel the molecular mechanism underlying the effects of *Dioscorea bulbifera Linn* (DB) on scopolamine-induced learning and memory impairment in ovariectomized (OVX) rats, with potential implications for Alzheimer's disease associated with estrogen changes in aging women. The prevalence of Alzheimer's disease, particularly in women, highlights the significance of understanding the role of estrogenic protection in AD pathogenesis. Despite the lack of well-established therapeutic interventions, our investigation sheds light on the potential of DB in memory deficit treatment. Through the integrated network pharmacology analysis, we identified multiple compounds, targets, and pathways that contribute to the neuroprotective effects of DB. One striking finding is the resemblance of DB's mechanism of action to estrogenic activity at a systems level, indicating that DB may mimic estrogen's protective effects. Our in vivo validation further confirmed the regulatory impact of DB on acetylcholine and estrogen expression. Importantly, we observed that DB extract at a dosage of 400 mg/kg BW/day demonstrated superior effects compared to estradiol, without any side effects, making it a promising alternative for managing age and gender-related toxicity on the cholinergic system. As we delve deeper into the pathway and explore the function of other proteins and mRNAs impacted by DB in AD, our results serve as a compelling starting point for future drug development efforts. With DB showcasing its potential as an adjuvant alongside standard AD treatment and as a nutraceutical supplement for menopausal females, our study opens new avenues for addressing AD-related challenges. Our integrated approach not only unveils the molecular mechanism of DB but also highlights its therapeutic potential. We hope that these findings will propel further research in the field of AD drug development and pave the way for effective strategies to combat this debilitating disease. By addressing the complexities of Alzheimer's disease and its association with estrogen changes, DB emerges as a promising natural candidate in the pursuit of better treatments and enhanced quality of life for those affected by this devastating condition.

Acknowledgments

The authors gratefully acknowledge the Department of Biotechnology, National Institute of Technology, Andhra Pradesh, India for providing us with the research facilities and funding. The R&D Facility at the Institute of Medical Sciences, Banaras Hindu University, and the Computational facility at the Department of Bioinformatics, Pondicherry University duly acknowledged.

Author Contributions

MRC & ATparticipated in conceptualization, manuscript preparation, network pharmacological analysis, and animal experimentation. MRC & KK performed molecular docking studies and analyses. GPD, BKT, and VSD designed the study, supervised the study process, and revised and edited the manuscript. All authors contributed toward data analysis, drafting, and critically revising the paper, gave final approval of the version to be published, and agree to be accountable for all aspects of the work.

Data availability

Data available in the article's supplementary material.

Ethical approval

The experimental study was approved by the institutional animal ethical committee, Institute of medical science, Banaras Hindu University, Varanasi U.P, India.

References

1. Adeniran, A. A. , and Sonibare, M. A. *2018. "Assessment of Genetic Fidelity of Dioscorea Bulbifera L. and Dioscorea Hirtiflora Benth. and Medicinal Bioactivity Produced from the Induced Tuberous Roots." Plant Cell, Tissue and Organ Culture (PCTOC) 132(2): 343–357. [Article] [Crossref][PubMed][Google Scholar]*

2. Adeosun, O. M. , Arotupin, D. J. *, Toba, O. A., and Adewole, A. 2016. "Antibacterial Activities and Phytochemical Properties of Extracts of Dioscorea Bulbifera Linn (Air Potatoe) Tubers and Peels against Some Pathogenic Bacteria." International Journal of Pharmaceutical Sciences and Research (IJPSR) 5(1): 20–22 [Crossref][PubMed][Google Scholar]*

3. Andrew, M. K. , and Tierney, M. C. *2018. "The Puzzle of Sex, Gender and Alzheimer's Disease: Why Are Women More Often Affected than Men?" Alzheimer's & Dementia [Crossref][PubMed][Google Scholar]*

4. Bisht, N. , Choudary, A. , Kumar, A. , and Kothiyal, P. *2013. "Evaluation of Therapeutic Potential of Dioscorea Bulbifera Tubers on Learning and Memory Impairment in..." International Journal of Advances in Pharmacy, Biology and Chemistry (IJAPBC) 2(12): 808–823 [Crossref][PubMed] [Google Scholar]*

5. Buckingham, S. D. , Jones, A. K. *, Brown, L. A., and Sattelle, D. B. 2009. "Nicotinic Acetylcholine Receptor Signalling: Roles in Alzheimer's Disease and Amyloid Neuroprotection." Journal of Neurochemistry 61(1): 39–61 [Crossref][PubMed] [Google Scholar]*

6. Cai, B. , et al. 2020. "Review Article Therapeutic Potential of Diosgenin and Its Major Derivatives against Neurological Diseases: Recent Advances. " *[Crossref][PubMed][Google Scholar]*

7. Cai, Z. 2014. "Monoamine Oxidase Inhibitors: Promising Therapeutic Agents for Alzheimer's Disease (Review). ". *[Crossref][PubMed][Google Scholar]*

8. Cerny, K. L. , Ribeiro, R. A. *C., Jeoung, M., and Ko, C. 2016. "Estrogen Receptor Alpha (ESR1)-Dependent Regulation of the Mouse Oviductal Transcriptome." [Crossref][PubMed][Google Scholar]*

9. Chandran, U. , Mehendale, N. , Patil, S. , and Chaguturu, R. *2020. "Network Pharmacology." [Crossref][PubMed][Google Scholar]*

10. Chaniad, P. , et al. 2020. "Anti-inflammatory, wound healing and antioxidant potential of compounds from Dioscorea bulbifera L. *bulbils." PLOS ONE 15(12): e0243632. [Article][Crossref] [PubMed][Google Scholar]*

11. Cholerton, B. , et al. 2002. "Estrogen and Alzheimer's Disease: The Story So Far. " *Journal of Neurochemistry 19(6): 405–427 [Crossref] [PubMed][Google Scholar]*

12. Crews, L. , and Masliah, E. 2010. "Molecular Mechanisms of Neurodegeneration in Alzheimer's Disease. " *Human Molecular Genetics 19(1): 12–20 [Crossref][PubMed][Google Scholar]*

13. Daina, A. , Michielin, O. , and Zoete, V. 2017. *"SwissADME: a free web tool to evaluate pharmacokinetics, drug-likeness and medicinal chemistry friendliness of small molecules." Scientific Reports 7: 42717. [Article][Crossref][PubMed] [Google Scholar]*

14. Daina, A. , Michielin, O. , and Zoete, V. 2019. *"SwissTargetPrediction: Updated Data and New Features for Efficient Prediction of Protein Targets of Small Molecules." Journal of Chemical Information and Modeling 47(May): 357–364 [Crossref] [PubMed][Google Scholar]*

15. Defina, P. A. , et al. 2013. *"Alzheimer's Disease Clinical and Research Update for Health Care Practitioners." Medical Clinics of North America 97(March): 1–11 [Crossref][PubMed][Google Scholar]*

16. Deroo, B. J. , and Korach, K. S. *2006. "Review Series Estrogen Receptors and Human Disease." Journal of Clinical Investigation 116(3): 561–570 [Crossref][PubMed][Google Scholar]*

17. Dubey, G. P. , et al. 2015. *"Combination treatment with a novel polyherbal formulation and metformin: a single blind placebo-controlled study in patients with T2DM and cognitive impairments." Diabetes 1(4): 92-102 [Crossref][PubMed][Google Scholar]*

18. Engvall, E. , and Perlmann, P. 1971. "Enzyme-linked immunosorbent assay (ELISA) quantitative assay for immunoglobulin G. " *Immunochemistry 8: 871 [Crossref][PubMed][Google Scholar]*

19. Fonseka, P. , et al. 2021. "FunRich Enables Enrichment Analysis of OMICs Datasets. " *Journal of Molecular Biology 433(11):166747. [Article] [Crossref][PubMed][Google Scholar]*

20. Ghosh, S. , et al. 2013. "Phytochemical Analysis and Free Radical Scavenging Activity of Medicinal Plants Gnidia Glauca and Dioscorea Bulbifera. " *Journal of Pharmacognosy and Phytochemistry 8(12): 1–18 [Crossref][PubMed][Google Scholar]*

21. Hebert, L. E. , et al. 2001. "*Is the Risk of Developing Alzheimer's Disease Greater for Women than for Men?" American Journal of Epidemiology 153(2): 132–136 [Crossref][PubMed][Google Scholar]*

22. Huang, L. , et al. 2018. "TCMID 2. *0: A Comprehensive Resource for TCM." Nucleic Acids Research 46(November 2017): 1117–1120 [Crossref][PubMed][Google Scholar]*

23. Jayachandran, K. S. , Vasanthi, H. R. *, and Rajamanickam, G. V. 2010. "Flavonoid Rich Fraction of Dioscorea Bulbifera Linn. (Yam) Enhances Mitochondrial Enzymes and Antioxidant Status, Thereby Protects Heart from Isoproterenol Induced Myocardial Infarction." [Crossref][PubMed][Google Scholar]*

24. Jesus, M. , Martins, A. P. J. *, Gallardo, E., and Silvestre, S. 2016. "Diosgenin: Recent Highlights on Pharmacology and Analytical Methodology." [Crossref][PubMed][Google Scholar]*

25. Kim, S. , et al. 2021. "PubChem in 2021: New Data Content and Improved Web Interfaces. *" Nucleic Acids Research 49, D1 (2021): D1388-D1395. [Article][Crossref][PubMed][Google Scholar]*

26. Knopman, D. S. , et al. 2021. *"Alzheimer Disease." Mayo Clinic Proceedings 7(1): 1–47 [Crossref][PubMed][Google Scholar]*

27. Komada, M. , Takao, K. , and Miyakawa, T. 2008. *"Elevated Plus Maze for Mice." [Crossref] [PubMed][Google Scholar]*

28. Kumar, S. , Das, G. , Shin, H. -S. *, and Patra, J. K. 2017. "Dioscorea Spp. (A Wild Edible Tuber): A Study on Its Ethnopharmacological Potential and Traditional Use by the Local People of Similipal Biosphere." [Crossref][PubMed][Google Scholar]*

29. Le, A. , et al. 2006. "Bafoudiosbulbins A, and B, Two Anti-Salmonellal Clerodane Diterpenoids from Dioscorea Bulbifera L. *Var Sativa." [Crossref] [PubMed][Google Scholar]*

30. Li, L. , et al. 2014. "Ovariectomy Results in Variable Changes in Nociception, Mood and Depression in Adult Female Rats. *" [Crossref] [PubMed][Google Scholar]*

31. Lipinski, C. A. , Lombardo, F. , Dominy, B. *W., and Feeney, P. J. 2001. "Experimental and Computational Approaches to Estimate Solubility and Permeability in Drug Discovery and Development Settings." Journal of Molecular Biology 46: 3–26 [Crossref][PubMed][Google Scholar]*

32. Liu, T. , et al. 2007. "BindingDB: A Web-Accessible Database of Experimentally Determined Protein–Ligand Binding Affinities. *" Nucleic Acids Research 35(December 2006): 198–201 [Crossref] [PubMed][Google Scholar]*

33. Lloret, A. , and Vi, J. 2010. "Why Women Have More Alzheimer's Disease Than Men: Gender and Mitochondrial Toxicity of Amyloid-β Peptide REACTIVE OXYGEN SPECIES IN THE. *" Current Alzheimer Research 20: 527–533 [Crossref] [PubMed][Google Scholar]*

34. Patel, D. , and Galani, V. J. 2017. *"Evaluation of Neuropharmacological Activity of Dioscorea Bulbifera Using Various Experimental Models." Journal of Pharmacy and Bioallied Sciences 7(1): 214–219 [Crossref][PubMed][Google Scholar]*

35. Malode, U. G. , et al. 2015. *"Phytochemical Investigations of Dioscorea Bulbifera Linn." International Journal of Pharmacy and Pharmaceutical Sciences 7(2): 20–23 [Crossref] [PubMed][Google Scholar]*

36. Maron, R. , et al. 2020. "Peptide Interference with APP and Tau Association: Relevance to Alzheimer's Disease Amelioration. *" [Crossref] [PubMed][Google Scholar]*

37. Merlo, S. , and Spampinato, S. F. 2017. *"Author's Accepted Manuscript." European Journal of Pharmacology [Crossref][PubMed][Google Scholar]*

38. Mitsushima, D. , et al. 2009. "Gonadal Steroids Maintain 24 h Acetylcholine Release in the Hippocampus: Organizational and Activational Effects in Behaving Rats. *" Journal of Neuroscience 29(12): 3808–3815 [Crossref][PubMed][Google Scholar]*

39. Musicco, Massimo. 2009. "Gender Differences in the Occurrence of Alzheimer's Disease. " Neurological Sciences 24(2): 2009. *[Crossref] [PubMed][Google Scholar]*

40. Noor, F. , et al. 2022. "Network Pharmacology Approach for Medicinal Plants: Review and Assessment. *" [Crossref][PubMed][Google Scholar]*

41. Padhan, B. , and Panda, D. 2020. "Potential of Neglected and Underutilized Yams (Dioscorea spp. *) for Improving Nutritional Security and Health Benefits." Frontiers in Plant Science 11(April): 1–13 [Crossref][PubMed][Google Scholar]*

42. Pi, J. , et al. 2020. "The DisGeNET Knowledge Platform for Disease Genomics: 2019 Update. *" Nucleic Acids Research 48(November 2019): 845–855 [Crossref][PubMed][Google Scholar]*

43. Ristic, N. , Živanovic, J. , and Šošic, B. 2014. *"Diosgenin Does Not Express Estrogenic Activity: A Uterotrophic Assay." Toxicology Letters 298(February): 292–298 [Crossref][PubMed] [Google Scholar]*

44. Roy, J. , et al. 2021. "Regulation of Melatonin and Neurotransmission in Alzheimer's Disease. *" [Crossref][PubMed][Google Scholar]*

45. Ru, J. , et al. 2014. "TCMSP: A Database of Systems Pharmacology for Drug Discovery from Herbal Medicines. *" Journal of Cheminformatics 6(1): 1–6 [Crossref][PubMed][Google Scholar]*

46. Sadhu, A. , Upadhyay, P. , and Agrawal, A. 2014. *"Management of Cognitive Determinants in Senile Dementia of Alzheimer's Type: Therapeutic Potential of a Novel Polyherbal Drug Product." [Crossref][PubMed][Google Scholar]*

47. Shannon, P. , et al. 2003. "Cytoscape: A Software Environment for Integrated Models of Biomolecular Interaction Networks. *" [Crossref] [PubMed][Google Scholar]*

48. Simone, A. D. , et al. 2021. *"Glycogen Synthase Kinase 3β: A New Gold Rush in Anti-Alzheimer's Disease Multitarget Drug Discovery?" [Crossref] [PubMed][Google Scholar]*

49. Small, D. H. , Avila, J. , and Sáez-Valero, J. *2011. "Revisiting the Role of Acetylcholinesterase in Alzheimer's Disease: Cross-Talk with P-Tau and β-Amyloid." Frontiers in Molecular Neuroscience 4(September): 1–9 [Crossref][PubMed][Google Scholar]*

50. Szklarczyk, D. , et al. 2021. "The STRING Database in 2021: Customizable Protein–Protein Networks, and Functional Characterization of User-Uploaded Gene/Measurement Sets. *" Nucleic Acids Research 49(November 2020): 605–612 [Crossref] [PubMed][Google Scholar]*

51. Upadhyay, P. , et al. 2018. "Revalidation of the Neuroprotective Effects of a United States Patented Polyherbal Formulation on Scopolamine-Induced Learning and Memory Impairment in Rats. *" Biomedicine & Pharmacotherapy 97(11): 1046–1052 [Crossref][PubMed][Google Scholar]*

52. Voller, A. , Bidwell, D. , & Bartlett, A. 1976. *"Microplate Enzyme Immunoassays for the Immunodiagnosis of Viral Infections." In: Manual of Clinical Immunology, ed. by N. Rose and H. Freedman, p. 506. American Society of Microbiology, Washington, D.C [Crossref][PubMed] [Google Scholar]*

53. Walczak-Nowicka, Ł. J. , and Herbet, M. 2021. *"Acetylcholinesterase Inhibitors in the Treatment of Neurodegenerative Diseases and the Role of Acetylcholinesterase in Their Pathogenesis." [Crossref][PubMed][Google Scholar]*

54. Wang, C. , et al. 2016. "Estrogen Receptor-α Is Localized to Neurofibrillary Tangles in Alzheimer's Disease. *" [Crossref][PubMed][Google Scholar]*

55. Yue, X. , et al. 2005. "Brain Estrogen Deficiency Accelerates Aβ Plaque Formation in an Alzheimer's Disease Animal Model. *" [Crossref][PubMed][Google Scholar]*

56. Zhu, D. , Montagne, A. , and Zhao, Z. 2021. *"Alzheimer's Pathogenic Mechanisms and Underlying Sex Difference." Cellular and Molecular Life Sciences 78(11): 4907–20. [Article][Crossref][PubMed] [Google Scholar]*

Disclaimer / Publisher's Note: The statements, opinions and data contained in all publications are solely those of the individual author(s) and contributor(s) and not of Journals and/or the editor(s). Journals and/or the editor(s) disclaim responsibility for any injury to people or property resulting from any ideas, methods, instructions or products referred to in the content.